PHASED ARRAY WITH NON-IDEAL DOUBLE PHASE SHIFTERS FOR MULTI-TARGET VITAL SIGN MONITORING

Zhaoyi Xu, Donglin Gao, Shuping Li, Chung-Tse Michael Wu and Athina Petropulu

Dept. of Electrical and Computer Engineering, Rutgers University

2024 IEEE International Symposium on Biomedical Imaging (ISBI) | 979-8-3503-1333-8/24/$31.00 ©2024 IEEE | DOI: 10.1109/ISBI56570.2024.10635792

ABSTRACT

A phased array equipped with double phase shifters (DPS) can reduce interference and enable multi-target vital sign monitoring (VSM) based on a single receive antenna. The DPS-phased array can control both the magnitude and the phase of the signal transmitted by each antenna, allowing for flexibly creating a desired beampattern. We consider the DPS-phased array weight design problem, taking into account practical constraints on the phase shifters, such as deviations from the nominal phases and insertion loss. The weights of practical phase shifters are selected so that the resulting DPS-phased array performs as close as possible to an ideal beamformer and transmits maximum power in the desired direction. The proposed design's effectiveness is demonstrated in experiments where the transmit power is focused on a specific human target to monitor corresponding vital signs. Simultaneously, an adjacent but unwanted human target is effectively nullified.

Index Terms— Remote Vital Sign Monitoring, Phased Array, Double Phase Shifters.

1. INTRODUCTION

In comparison to traditional monitoring methods that depend on body-attached sensors, remote vital sign monitoring (VSM) is less intrusive and does not necessitate the subject's cooperation [1]. Remote VSM has been studied for many applications including diagnosis and observation of obstructive apnea [2], noncontact infant breathing rate (BR) and heartbeat rate (HR) monitoring [3] and driver drowsiness detection [4].

Phased arrays have been widely investigated for remote VSM due to their simple design and cost-effectiveness [5, 6]. A typical phased array comprises a single radio frequency (RF) chain and multiple transmit antennas, each linked to the RF chain through a phase shifter. The phased array achieves beamforming by adjusting the phases of these shifters. However, due to its inability to control the magnitude of the signal transmitted by each antenna, the phased array lacks the flexibility to attain a desired beampattern. This limitation becomes problematic in multi-target scenarios, where undesired targets may also be excited. In that case, when using a single antenna receiver, the unwanted targets create interference impeding the VSM of the desired target. To address this issue, one could use an active electronically scanned array (AESA) where each antenna connects to the RF chain through a transmit/receive module [7] or a multiple-input multiple-output (MIMO) radar where each antenna is equipped with an RF chain [8]. Both allow for control over both magnitude and phase, however, they also significantly raise the overall cost.

A phased array equipped with double phase shifters (DPS) has shown promise in bypassing the constant modulus (CM) challenges of the phase shifters with a modestly increased cost [9]. In our prior work [10], we constructed a DPS-phased array prototype and tested it on simulated subjects, i.e., actuators loaded with copper boards mimicking the human chest movement. We demonstrated that it can focus its power on the target of interest while suppressing the energy emitted towards undesired targets in proximity. However, in those experiments, the design assumes that the phase shifters are ideal, i.e., they all have the same unit-modulus weights.

This paper investigates DPS-phased array design based on non-ideal phase shifters. Practical phase shifters have discrete phases with limited phase resolution, and due to manufacturing errors, their phases exhibit discrepancies from the nominal values. Further, due to the inherent power loss of a phase shifter, known as insertion loss, the magnitude of the signal going through the phase shifter is also affected, with the effect varying between different phases of the same phase shifter and between different phase shifters. In [10], when ignoring those imperfections, the created nulls were not deep enough to fully eliminate the interference from the undesired target. Here, the weights of those practical phase shifters are selected so that the resulting DPS-phased array performs as close as possible to an ideal beamformer and at the same time delivers maximum power in the desired direction. We verify the effectiveness of the proposed design in remote VSM of a specific human target sitting in close proximity to another non-pertinent human target. The experimental results affirm that the DPS-phased array can focus the transmitted energy to the desired target, enabling good VSM performance, while nullifying the closely spaced undesired human target.

2. MOTIVATION FOR DPS-PHASED ARRAY

Let us consider a phased array equipped with an N-element uniform linear array (ULA) configuration with antenna

Work supported by NSF under grant ECCS-2033433 and ARO under grant W911NF2320103.

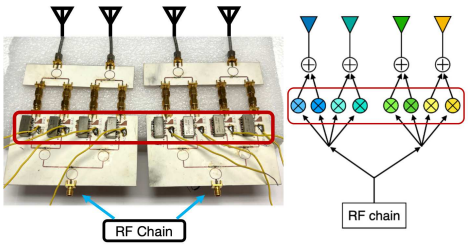

Fig. 1: DPS-phased array prototype (left) and its schematic (right). The phase shifters are in the wine circle.

spacing d. The array is fed with a unit-power baseband signal $e(t)$ with wavelength λ. The power radiated towards direction θ is $p(\mathbf{w},\theta) = \mathbf{a}^H(\theta)\mathbf{w}\mathbf{w}^H\mathbf{a}(\theta)$, where $\mathbf{a}(\theta) = [1, e^{j2\pi d\frac{\sin\theta}{\lambda}}, \ldots, e^{j2\pi(N-1)d\frac{\sin\theta}{\lambda}}]^T$ is the steering vector in direction θ; $(\cdot)^H$ denotes conjugate transpose; and $\mathbf{w} \in \mathbb{C}^{N\times 1}$ is the weight vector. On setting $\mathbf{w} = \mathbf{a}(\theta_0)$, where θ_0 is the direction of the desired target, the signals transmitted by the antennas will add up coherently at θ_0. However, such a beamformer does not offer any control of the transmit beam sidelobes, allowing the transmit power to reach directions other than θ_0 and excite targets of no interest.

To mitigate the interference from the undesired targets and suppress the sidelobes, one needs to solve the problem

$$\begin{aligned} \min_{\mathbf{w}} \quad & \sum_{i=1}^{I} p(\mathbf{w},\theta_i) \\ \text{s.t.} \quad & p(\mathbf{w},\theta_0) = 1, \text{ and } w_n \in \mathcal{S}_n, \quad n = 1,\ldots,N. \end{aligned} \tag{1}$$

where $\{\theta_1,\ldots,\theta_I\}$ contains the directions to be nullified, and w_n and $\mathcal{S}_n$ are respectively the weight of the n-th antenna and the corresponding feasible set.

For a phased array with ideal phase shifters, the feasible sets contain complex numbers subject to a CM constraint and are non-convex which makes (1) hard to solve. One way to deal with the non-convexity is to approximate the objective function using Taylor expansion. The new problem is convex, but also yields a sub-optimal solution and a degraded beampattern shaping performance [11]. Further, the solution in [11] requires substantial computation effort to iteratively update the unit-modulus antenna weights.

In a DPS-phased array [9], each antenna is equipped with two phase shifters (see the right part of Fig. 1). Any complex number with magnitude $|M| \leq 2$ can be uniquely decomposed into two unit-modulus numbers [12], i.e.,

$$Me^{j\omega} = e^{j\phi_1} + e^{j\phi_2}, \quad |M| \leq 2, \tag{2}$$

where $\omega = (\phi_1+\phi_2)/2$ and $M = 2\cos((\phi_1-\phi_2)/2)$. Therefore, one can first solve (1) without worrying about CM constraints, normalize the obtained weights to have a maximum magnitude of 2, and then decompose each weight into two unit-modulus numbers based on (2). In that way, the feasible set in a DPS-phased array consists of all complex numbers with a magnitude no larger than 2. The DPS-phased array involves a modest increase in hardware cost as compared to a phased array, stemming from the use of more phase shifters, which are nevertheless inexpensive.

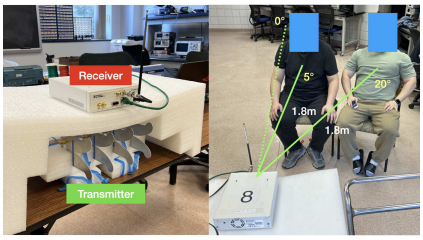

Fig. 2: Experiment setup.

3. DPS-PHASED ARRAY WITH NON-IDEAL PHASE SHIFTERS

In a DPS-phased array with practical phase shifters, the feasible set corresponding to the n-th antenna, $\mathcal{S}_n$, can be described as $\{s_k \in \mathcal{S}_n | s_k = a_i + b_j, a_i \in \mathcal{A}_n, |a_i| < 1,\ b_j \in \mathcal{B}_n, |b_j| < 1,\ \forall i,j\}$ where $\mathcal{A}_n$ and $\mathcal{B}_n$ contain the weights of the two phase shifters linked to the n-th antenna and their elements are different. The optimization problem in (1) resembles a mixed-integer programming (MIP) problem as each variable is taken from a specific complex set with limited size. To efficiently solve a MIP problem, we first relax the feasible set constraint which provides a convex problem with a globally optimal solution, and then approximate the optimal solution by using weights from the feasible set [13]. Without the feasible set constraint, the solution of (1) is the well-known minimum variance distortionless response (MVDR) beamformer, and when $p(\mathbf{w},\theta_i) = 0, \forall i \neq 0$, the solution is the null-steering beamformer [14]. Due to the insertion loss, the elements in $\mathcal{S}_n$ have a small magnitude. Thus the optimal beamformer needs to be normalized such that its elements are close to the elements in the feasible set. Let the optimal solution be denoted by $\mathbf{w}^\dagger$. Suppose that the m-th element of $\mathbf{w}^\dagger$ has the largest magnitude and s_{max} is the element with the largest magnitude in $\mathcal{S}_m$. The weight design problem can be formulated as

$$\begin{aligned} \min_{\mathbf{w}} \quad & \|\mathbf{w} - \alpha\mathbf{w}^\dagger\|_2^2 \\ \text{s.t.} \quad & \gamma \leq |\alpha| \leq |\frac{s_{max}}{w_m^\dagger}| \text{ and } w_n \in \mathcal{S}_n, n = 1,\ldots,N. \end{aligned} \tag{3}$$

where α is a complex coefficient whose magnitude determines the level of insertion loss; $\|\cdot\|_2$ is the ℓ_2 norm; and $\gamma \in (0, |s_{max}/w_m^\dagger|]$ is a predefined threshold. With ideal phase shifters, the optimal beamformer can be approximated well using a real α, as described in Sec. 2. For non-ideal phase shifters, however, one needs to properly choose a complex α to scale the magnitude and change the phase of $\mathbf{w}^\dagger$.

Solving (3) still involves a lot of computations. To efficiently solve (3), we aim to maximize the magnitude of α to minimize the insertion loss and thus maximize the transmit power, i.e., by letting $\alpha = \gamma = s_{max}/w_m^\dagger$. However, the corresponding solution may have a poor approximation performance. To tackle this issue, we divide the feasible set $\mathcal{S}_m$ into K subsets based on the phase of its elements, and for each subset, we find the solution that maximizes $|\alpha|$. In

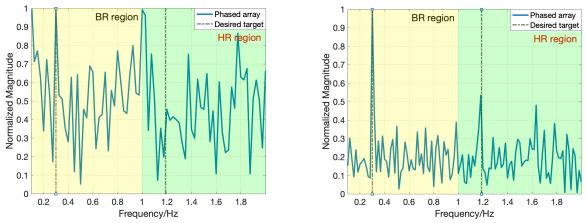

(a) (b)

Fig. 3: Single-target VSM results via a phased array. The desired target is at 5° in (a) and -10° in (b).

particular, for each subset $\mathcal{S}_m^k$, we find the element with the largest magnitude, i.e., s_m^k, based on which, the complex coefficient is taken as $\alpha_k = s_m^k / w_m^\dagger$. Then for the rest of $N-1$ elements, we compute $\alpha_k w_n^\dagger$ and based on its phase, we find the corresponding subset $\mathcal{S}_n^{k'}$ and the closest element within $\mathcal{S}_n^{k'}$. Finally, we compare the K solutions and choose the best one with respect to the predefined criteria, e.g., the null depth.

4. VITAL SIGN ESTIMATION USING A DPS-PHASED ARRAY

To fully nullify the undesired targets while focusing the radiated power on the target of interest, we use the null-steering beamformer $\mathbf{w}_{ns} = \mathbf{P}\mathbf{a}(\theta_0)$, where $\mathbf{P} = \mathbf{I}_N - \mathbf{A}(\mathbf{A}^H\mathbf{A})^{-1}\mathbf{A}^H$ is the orthogonal projection matrix, $\mathbf{I}_N$ is an $N \times N$ identity matrix and $\mathbf{A} \in \mathbb{C}^{N\times I}$ contains the steering vectors corresponding to the I nulls. As we only investigate the beampattern synthesis performance of the DPS-phased array, we will use a simple continuous-wave (CW) signal $e(t) = e^{j2\pi(f_c t + \phi_0 + \Delta\phi(t))}$ as the baseband signal where f_c is the carrier frequency, ϕ_0 is the initial phase and $\Delta\phi(t)$ is the time-varying phase noise. The received signal is given as

$$y(t) = \sum_{i=0}^{I} \beta_i \mathbf{a}^H(\theta_i)\mathbf{w}_{ns} e(t - \tau_i(t)) + n(t) \qquad (4)$$

where the complex coefficient β_i accounts for the path loss and radar cross section (RCS) of the i-th target, $\tau_i(t)$ is the round-trip delay of the i-th target, and $n(t)$ consists of random noise and reflections from the static environment. The round-trip delay of the i-th target $\tau_i(t) = \frac{2R_i + R_i(t)}{c}$ is associated with nominal distance R_i and changes with the chest wall movement $R_i(t)$. Assume that the implemented complex weights $\mathbf{w}_{ns}$ fully nullify the undesired targets and focus the energy on the target of interest. After mixing the received signal with the conjugate of the baseband signal, we can write the mixed signal as

$$s(t) = y(t)e^*(t) = \beta_0' A e^{-j2\pi\frac{R_0(t)}{\lambda}} + n'(t) \qquad (5)$$

where $\beta_0' = \beta_0 e^{j2\pi 2R_0/\lambda}$, A is a real coefficient accounting for the array gain with insertion loss and $n'(t) = n(t)x^*(t)$. Note that, since the phase noise is slow-varying, the phase noise term is canceled in (5).

The chest displacement $R_0(t)$ is now encoded in the phase of the mixed signal $s(t)$, which can be approximated as

$$R_0(t) \approx A_b \sin(2\pi f_b t + \phi_b) + A_h \sin(2\pi f_h t + \phi_h) \qquad (6)$$

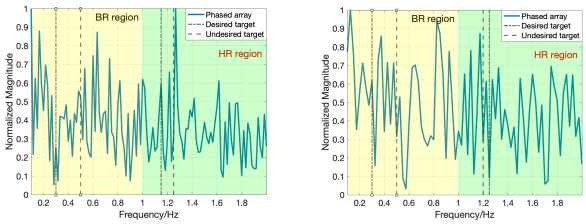

(a) (b)

Fig. 4: Multi-target VSM results via a phased array. The desired and undesired targets are respectively at: $(5^\circ, 20^\circ)$ in (a) and $(-10^\circ, 10^\circ)$ in (b).

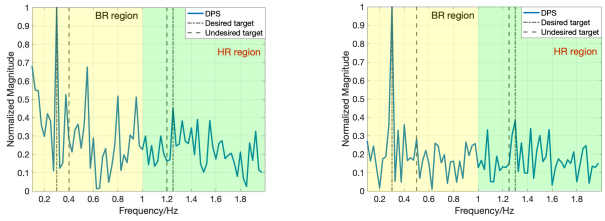

(a) (b)

Fig. 5: Multi-target VSM results via a DPS-phased array. The desired and undesired targets are respectively at: $(5^\circ, 20^\circ)$ in (a) and $(-10^\circ, 10^\circ)$ in (b).

where A_b, f_b and ϕ_b are respectively the amplitude, frequency, and initial phase of the chest movement due to breathing and A_h, f_h and ϕ_h are the corresponding parameters related to heartbeat. By dividing the mixed signal into I/Q signals and applying arctangent demodulation, the phase of $s(t)$ can be extracted. Consequently, by applying a discrete Fourier transform (DFT) on those phases, one can estimate the frequency components of $R_0(t)$, i.e., f_b and f_h.

5. EXPERIMENT RESULTS

Here we use the DPS-phased array prototype [10] shown in Fig. 1 which has 8 phase shifters whose weights are controlled by the applied voltage. A vector network analyzer (VNA) was used to measure the weights in each phase shifter by varying the applied voltage from 0 V to 15 V with a 0.2 V step size. A 2.2 GHz CW signal generator with a signal amplifier was used as the signal source, and four Vivaldi antennas were employed as transmit antennas. Simultaneously, a commercial software-defined radio (SDR) device USRP-2920 equipped with an omnidirectional antenna was utilized as the receiver. The transmitter and receiver are shown on the left side of Fig. 2. The ground truth of HR was collected using two commercial contactable VSM devices while the targets were asked to breathe following two metronomes. Institutional review board (IRB) protocol approval of the experiments was acquired under study ID Pro2022001336.

In order to compare the performance between a conventional phased array and a DPS-phased array we conducted 3 experiments with different setups, i.e., i) phased array with a single target, ii) phased array with two targets, and iii) DPS-phased array with two targets. In each experiment, the radar-to-target distance is 1.8m. In the first two experiments, the transmitter worked as a phased array by only connecting one

phase shifter to each antenna. Each experiment is repeated with two different direction configurations: the desired target is at 5° or -10° and the undesired target (if it exists) is located at 20° or 10°, correspondingly. The target setup of the (5°,20°) case is illustrated on the right side of Fig. 2 where the green dashed line represents the direction of 0°.

In the first experiment, a phased array is used to measure the vital signs of a single target. The target was located in the desired direction and the results are shown in Fig. 3. As observed, the phased array can find the vital signs in the single-target scenario. However, in the 5° case (Fig. 3a), due to the non-ideal phase shifters and the limited number of transmit antennas, the beamforming performance is not good as the frequency spectrum is very noisy and a high peak appears at 1 Hz. When it comes to VSM in the multi-target scenario, the phased array fails to find the vital signs of the desired target, as shown in Fig. 4. Since the phased array cannot distinguish targets that are closely spaced, the vital signs of two targets are all extracted. As those frequencies mix with each other and also their corresponding harmonics, the resulting frequency spectrum becomes noise-like.

In the third experiment, the DPS-phased array is used to estimate the vital signs in the same multi-target scenario. The total number of weight combinations is more than 1×10^{15} while the proposed method only takes 0.03s to design the weights when $K = 4$. The estimation results are shown in Fig. 5 where the BR and HR of the desired target are successfully estimated and found in agreement with the ground truth. Compared to the conventional phased array, the DPS-phased array fully nullifies the closely spaced undesired target, while extracting the vital signs of the desired target. Furthermore, one can see that the DPS-phased array achieves better beamforming performance as the frequency spectrum in Fig. 5a is less noisy than that in Fig. 3a. Note that, when K is large, the DPS-phased array will have better beamforming and nullifying performance but may have a lower SNR.

6. CONCLUSION

We have addressed the DPS-phased array design with non-ideal phase shifters. Our experimental results in VSM of humans clearly demonstrate that the DPS-phased array effectively nullifies a neighboring target, allowing for VSM of the desired human target. It has also been experimentally shown that the vital signals extracted by the DPS-phased array have better SNR as compared to those extracted based on a conventional phased array in the same setup.

7. REFERENCES

[1] F.-K. Wang, C.-T. M. Wu, T.-S. Horng, C.-H. Tseng, S.-H. Yu, C.-C. Chang, P.-H. Juan, and Y. Yuan, "Review of self-injection-locked radar systems for noncontact detection of vital signs," *IEEE Journal of Electromagnetics, RF and Microwaves in Medicine and Biology*, 2020.

[2] V. P. Tran, A. A. Al-Jumaily, and S. M. S. Islam, "Doppler radar-based non-contact health monitoring for obstructive sleep apnea diagnosis: A comprehensive review," *Big Data and Cognitive Computing*, 2019.

[3] C. Li, J. Cummings, J. Lam, E. Graves, and W. Wu, "Radar remote monitoring of vital signs," *IEEE Microwave Magazine*, vol. 10, no. 1, pp. 47–56, 2009.

[4] H. U. R. Siddiqui, A. A. Saleem, R. Brown, B. Bademci, E. Lee, F. Rustam, and S. Dudley, "Non-invasive driver drowsiness detection system," *Sensors*, 2021.

[5] M. Nosrati, S. Shahsavari, S. Lee, H. Wang, and N. Tavassolian, "A concurrent dual-beam phased-array Doppler radar using MIMO beamforming techniques for short-range vital-signs monitoring," *IEEE Transactions on Antennas and Propagation*, vol. 67, no. 4, 2019.

[6] S. M. Islam, N. Motoyama, S. Pacheco, and V. M. Lubecke, "Non-contact vital signs monitoring for multiple subjects using a millimeter wave FMCW automotive radar," in *2020 IEEE/MTT-S International Microwave Symposium (IEEE IMS)*, 2020, pp. 783–786.

[7] N. J. Kolias and M. T. Borkowski, "The development of T/R modules for radar applications," in *2012 IEEE/MTT-S International Microwave Symposium Digest*, 2012, pp. 1–3.

[8] Z. Xu, C. Shi, T. Zhang, S. Li, Y. Yuan, C.-T. M. Wu, Y. Chen, and A. Petropulu, "Simultaneous monitoring of multiple people's vital sign leveraging a single phased-MIMO radar," *IEEE Journal of Electromagnetics, RF and Microwaves in Medicine and Biology*, 2022.

[9] Z. Xu and A. P. Petropulu, "Phased array with improved beamforming capability via use of double phase shifters," in *2022 IEEE 12th Sensor Array and Multichannel Signal Processing Workshop (SAM)*, 2022.

[10] Z. Xu, D. Gao, S. Li, C.-T. M. Wu, and A. Petropulu, "Flexible beam design for vital sign monitoring using a phased array equipped with double-phase shifters," in *2023 IEEE International Conference on Acoustics, Speech and Signal Processing (ICASSP)*, 2023.

[11] Y. Aslan, J. Puskely, A. Roederer, and A. Yarovoy, "Phase-only control of peak sidelobe level and pattern nulls using iterative phase perturbations," *IEEE Antennas and Wireless Propagation Letters*, 2019.

[12] X. Yu, J. Zhang, and K. B. Letaief, "Doubling phase shifters for efficient hybrid precoder design in millimeter-wave communication systems," *Journal of Communications and Information Networks*, 2019.

[13] P. Belotti, C. Kirches, S. Leyffer, J. Linderoth, J. Luedtke, and A. Mahajan, "Mixed-integer nonlinear optimization," *Acta Numerica*, vol. 22, Apr. 2013.

[14] B. Friedlander, "On transmit beamforming for MIMO radar," *IEEE Transactions on Aerospace and Electronic Systems*, vol. 48, no. 4, pp. 3376–3388, 2012.